

Mechanistic Insights into Hydrodeoxygenation of Phenol on Bimetallic Phosphide Catalysts

Varsha Jain,^a Yolanda Bonita,^b Alicia Brown,^{a‡} Anna Taconi,^{a‡} Jason C. Hicks,^b
and Neeraj Rai^{a*}

^a *Dave C. Swalm School of Chemical Engineering and Center for Advanced Vehicular Systems, Mississippi State University, Mississippi State, Mississippi 39762, United States.*

^b *Department of Chemical and Biomolecular Engineering, 182 Fitzpatrick Hall, University of Notre Dame, Indiana 46556, United States.*

‡ Authors AB and AT contributed equally.

E-mail: neerajrai@che.msstate.edu

Phone: (+1) 662-325-0790. Fax: (+1) 662-325-2482

X-ray diffraction (XRD) patterns

The crystal structures of the materials were confirmed using powder XRD in Figure 1. The XRD patterns of RuMoP, NiMoP, and FeMoP are plotted in Figure S1 (a), S1 (c), and S1(e) respectively with their corresponding reference pattern in Figure S1 (b), S1 (d), and S1 (f). The three most dominant peaks are marked with stars for the orthorhombic RuMoP and FeMoP, while the three most dominant peaks in NiMoP are marked with dots. The most dominant peak in FeMoP and RuMoP observed in XRD are (112) peak, while (111) facet is the most dominant in NiMoP samples. The XRD results confirmed that the materials are solid solution of bimetallic phosphides and are not mixtures.

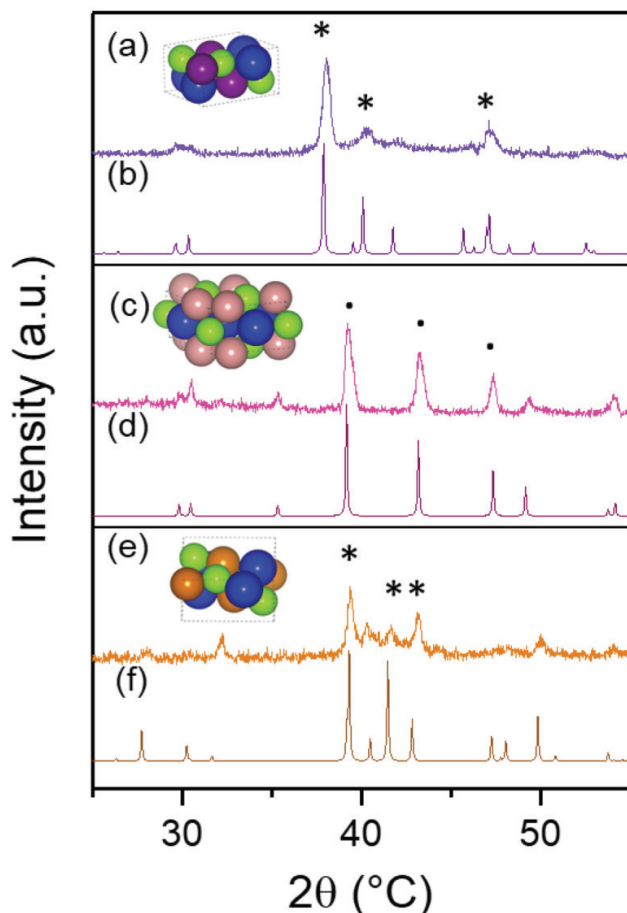


Figure S1: XRD pattern of (a) RuMoP (b) RuMoP reference pattern (PDF 04-015-7732) (c) NiMoP (d) NiMoP reference pattern (PDF 00-031-0873), (e) FeMoP (f) FeMoP reference pattern (PDF 04-001-4637).

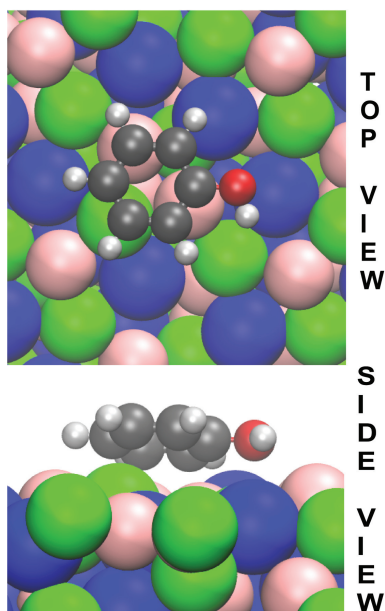


Figure S2: Adsorption of phenol (C_6H_5OH) on (111) facet of NiMoP catalyst.

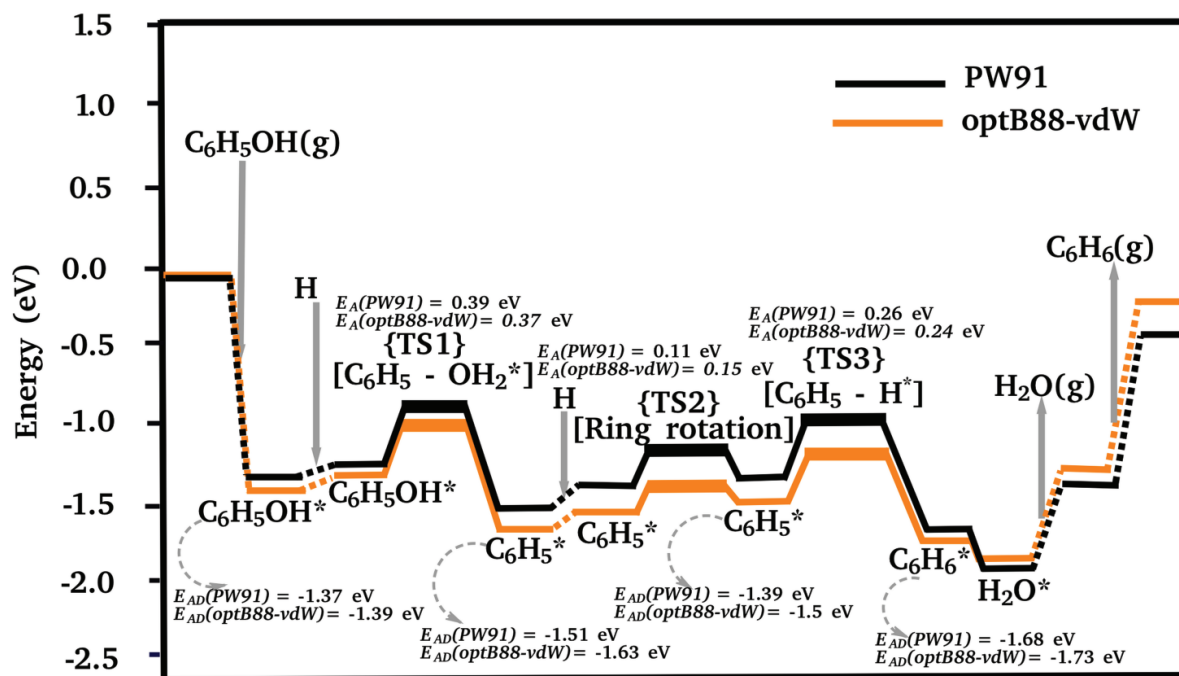


Figure S3: Reaction energetics on the (112) facet of FeMoP catalyst during DDO reaction. The black and orange colors represent results for PW91 and optB88-vdW functionals.

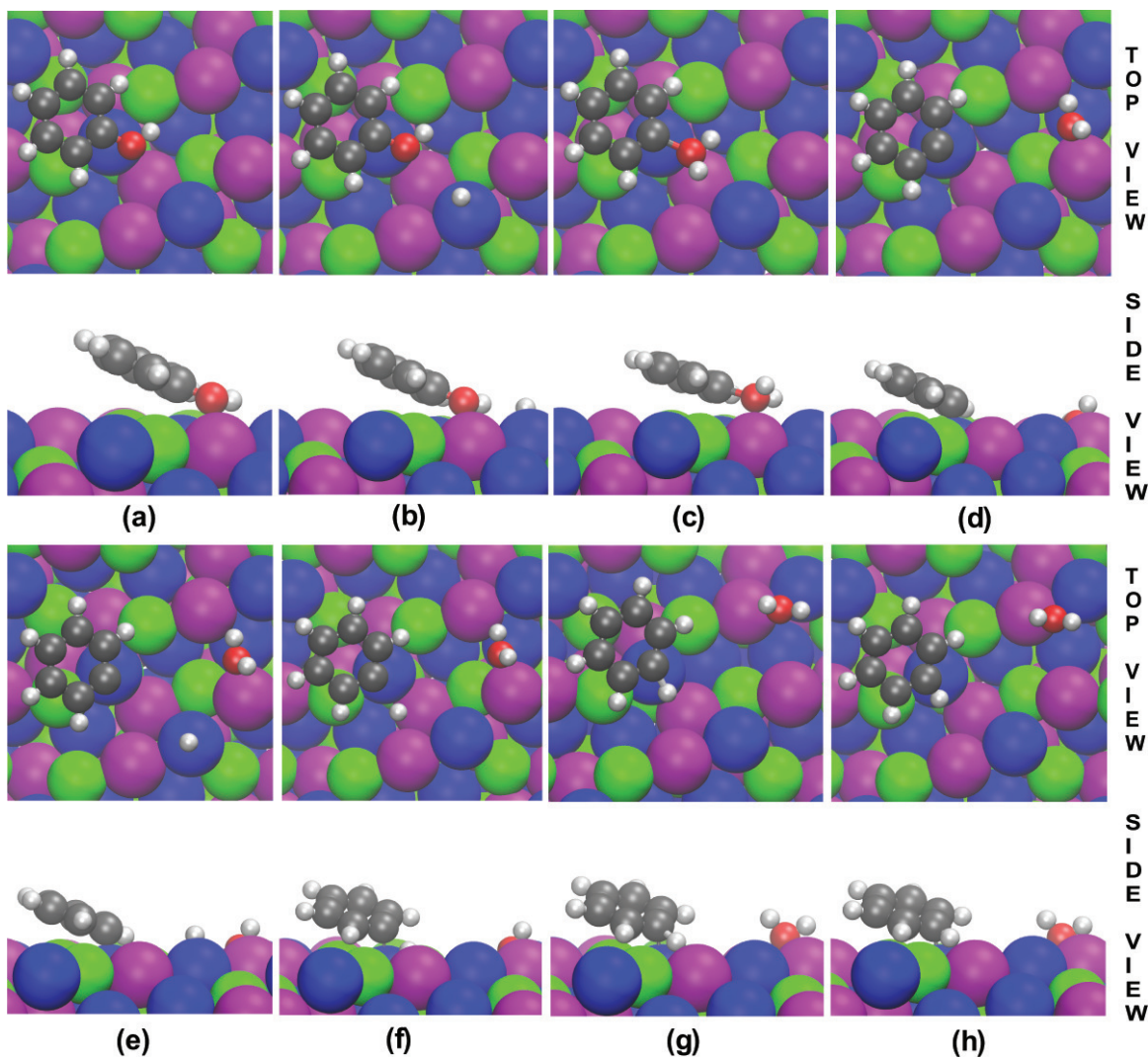


Figure S4: Optimized structures of phenol (C_6H_5OH), benzene (C_6H_6), and reaction intermediates on the (112) facet of RuMoP during DDO reaction: (a) $C_6H_5OH^*$, (b) $C_6H_5OH^*$ and H^* , (c) $C_6H_5-OH_2^*(TS1)$, (d) $C_6H_5^*$ and OH_2^* , (e) H^* , $C_6H_5^*$, and H_2O^* , (f) H^* , rotated $C_6H_5^*$, and H_2O^* , (g) $C_6H_5-H^*$ and $H_2O^*(TS3)$, and (h) $C_6H_6^*$ and H_2O^* . The purple, blue, and green colors represent Ru, Mo, and P atoms, respectively.

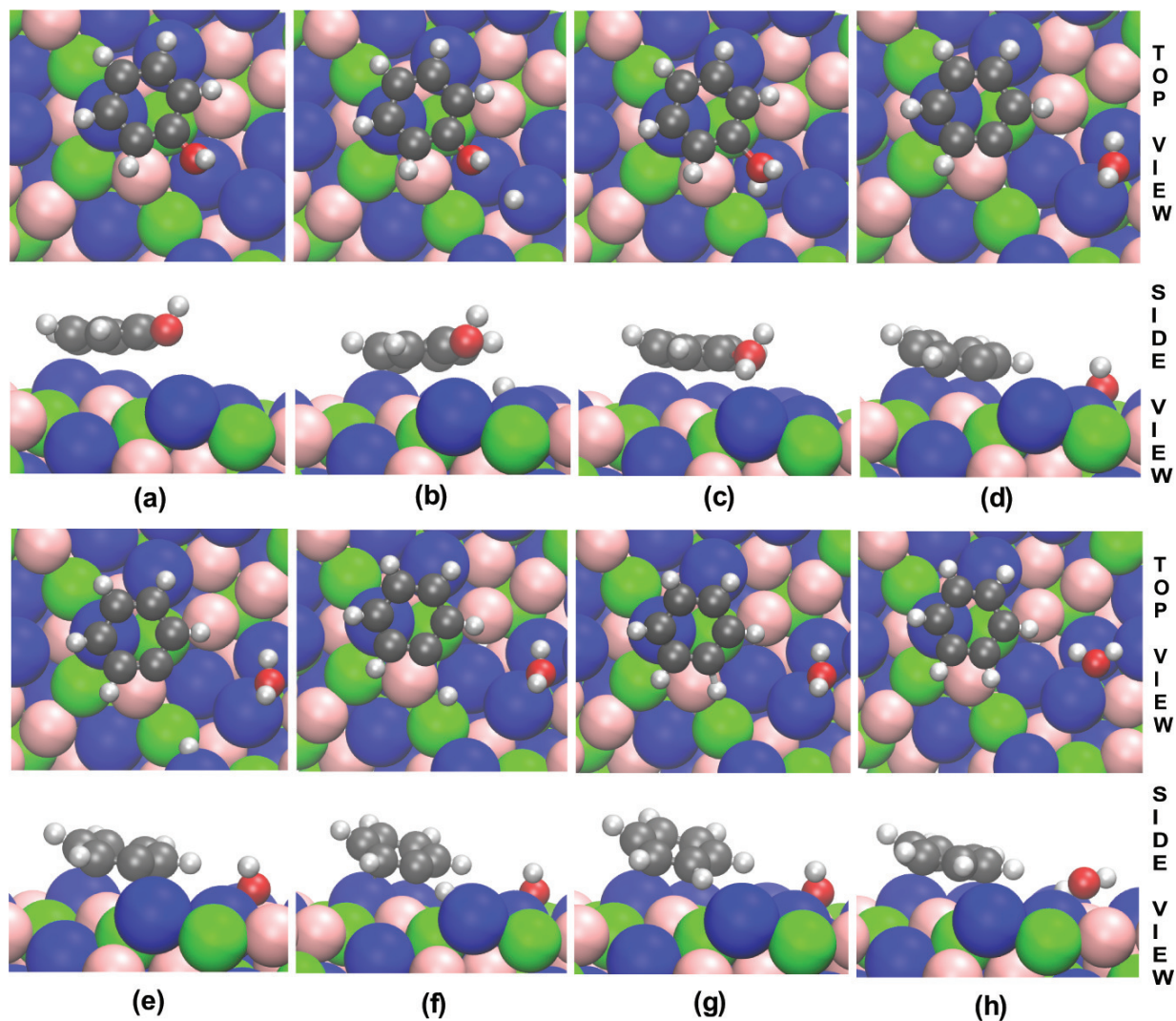


Figure S5: Optimized structures of phenol (C_6H_5OH), benzene (C_6H_6), and reaction intermediates on the (112) facet of NiMoP during DDO reaction: (a) $C_6H_5OH^*$, (b) $C_6H_5OH^*$ and H^* , (c) $C_6H_5-OH_2^*(TS1)$, (d) $C_6H_5^*$ and OH_2^* , (e) H^* , $C_6H_5^*$, and H_2O^* , (f) H^* , rotated $C_6H_5^*$, and H_2O^* , (g) $C_6H_5-H^*$ and $H_2O^*(TS3)$, and (h) $C_6H_6^*$ and H_2O^* . The pink, blue, and green colors represent Ni, Mo, and P atoms, respectively.

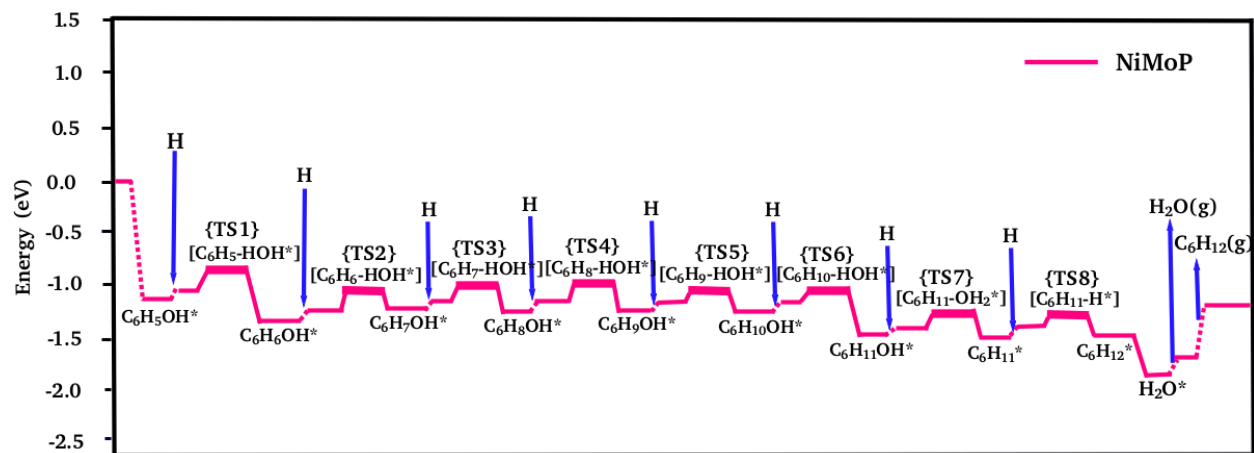


Figure S6: Reaction energetics on the (112) facet of NiMoP catalyst during RH-DO reaction.

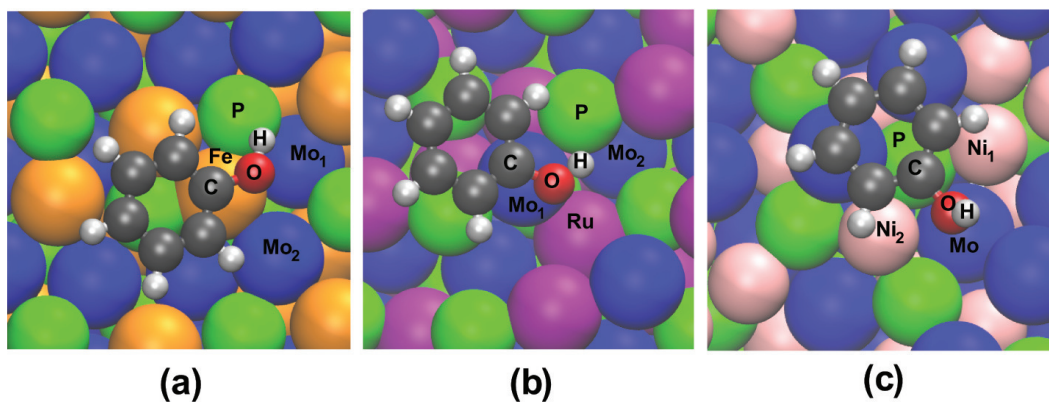


Figure S7: Atom numbering on (a) FeMoP and phenol, (b) RuMoP and phenol, (c) NiMoP and phenol systems for distance measurement in Table S7.

Table S1: Lattice vector lengths (\AA) of P (2×2) simulation cell of FeMoP, RuMoP, and NiMoP systems via optB88-vdW functional

system	a	b	c
FeMoP	11.78	12.95	29.43
RuMoP	14.32	20.75	21.99
NiMoP	13.87	24.59	21.99

Table S2: Effect of altering the k-points grid on adsorption energy (E_{AD} , eV) of phenol and activation energy barrier (E_A , eV) of C–O bond cleavage on (112) surface of FeMoP, RuMoP, and NiMoP, respectively

system	gamma point	E_{AD}		gamma point	E_A	
		2 X 2 X 1	4 X 4 X 1		2 X 2 X 1	4 X 4 X 1
FeMoP	-1.393	-1.393	-1.394	0.372	0.372	0.373
RuMoP	-1.291	-1.294	-1.296	0.484	0.482	0.482
NiMoP	-1.215	-1.212	-1.215	0.802	0.803	0.805

Table S3: Partial charges (q , $|e|$) on individual atom of phenol on the (112) facet of RuMoP catalyst by using different grid size (NGX, NGY, NGZ or NGXF, NGYF, NGZF) and PREC-flag

site	NG* = 80 X 108 X 120	160 X 216 X 240	80 X 108 X 120	100 X 144 X 160
	NG*F = 160 X 216 X 240	320 X 432 X 480	80 X 108 X 120	200 X 288 X 320
C ₁	+0.38	+0.40	+0.39	+0.37
C ₂	+0.21	+0.24	+0.20	+0.18
C ₃	- 0.18	- 0.18	- 0.19	- 0.18
C ₄	+0.13	+0.13	+0.13	+0.14
C ₅	- 0.22	- 0.22	- 0.22	- 0.23
C ₆	- 0.13	+0.14	- 0.13	+0.14
O	- 1.10	- 1.12	- 1.10	- 1.09
H	+0.77	+0.79	+0.76	+0.75

Table S4: Cell parameters (\AA) of FeMoP, RuMoP, and NiMoP system using 2 X 4 X 2 supercell size via optB88-vdW functional (experimental and computational comparison)

cell parameters	FeMoP		RuMoP		NiMoP	
	exp.	comp.	exp.	comp.	exp.	comp.
a	11.84	11.75	12.07	12.06	11.72	11.65
b	14.60	14.80	15.41	15.48	23.44	23.30
c	13.56	13.48	13.88	13.88	7.40	7.33

Table S5: Effect of simulation cell size on adsorption energies (E_{AD} , eV) of phenol ($\text{C}_6\text{H}_5\text{OH}$) on (112) facet of FeMoP, RuMoP, and NiMoP by using optB88-vdW functional

system	E_{AD} (P (2 X 2))	E_{AD} (P (4 X 4))
FeMoP	-1.392	-1.393
RuMoP	-1.291	-1.294
NiMoP	-1.211	-1.218

Table S6: Adsorption energies (E_{AD} , eV) of phenol ($\text{C}_6\text{H}_5\text{OH}$) and benzene (C_6H_6) on (112) and (111) facet of NiMoP catalyst by using optB88-vdW functional

molecule	E_{AD} (112 plane)	E_{AD} (111 plane)
phenol	-1.21	-1.26
benzene	-1.40	-1.45

Table S7: Distance (d , Å) between selected atoms of phenol (C_6H_5OH) and nearby surface atoms after adsorption on (112) facet of FeMoP, RuMoP, and NiMoP catalyst by using optB88-vdW functional (see Fig. S7 for atom numbering)

system	distance	d
FeMoP	C-Fe	2.13
	O-Fe	2.10
	O-Mo ₁	3.16
	O-Mo ₂	3.12
	O-P	2.40
	H-Fe	2.52
	H-Mo ₁	2.94
	H-P	1.75
RuMoP	C-Ru	4.26
	C-Mo ₁	2.5
	O-Ru	3.26
	O-Mo ₁	2.27
	O-Mo ₂	4.42
	O-P	3.02
	H-Ru	3.45
	H-Mo ₁	2.66
	H-Mo ₂	4.02
H-P	2.51	
NiMoP	C-Mo ₁	4.58
	O-Ni ₁	3.98
	O-Ni ₂	3.73
	O-Mo	4.32
	O-P	4.9
	H-Ni ₁	4.7
	H-Ni ₂	4.68
H-P	4.9	

Table S8: Adsorption energies (E_{AD} , eV) of H on top of Fe, Ru, Ni, Mo, P atoms and in between two neighboring atoms of (112) facet by using optB88-vdW functional

atom type	E_{AD}
Fe	- 0.11
Ru	- 0.07
Ni	- 0.09
Mo	- 0.18
P	- 0.02
Fe-Mo	- 0.16
Ru-Mo	- 0.12
Ni-Mo	- 0.12
Fe-P	- 0.08
Ru-P	- 0.06
Ni-P	- 0.08
Mo-P	- 0.10

Table S9: Activation energy barriers (E_A , eV) of main elementary reaction steps involved in DDO reaction mechanism for phenol on (112) facet of FeMoP, RuMoP, and NiMoP catalyst for different DFT functionals

reaction steps	FeMoP		RuMoP		NiMoP	
	optB88-vdW	PW91	optB88-vdW	PW91	optB88-vdW	PW91
C-O cleavage	0.37	0.39	0.48	0.54	0.8	0.98
ring rotation	0.15	0.11	0.21	0.18	0.28	0.27
C-H formation	0.24	0.26	0.28	0.33	0.89	1.1

Table S10: Partial charges (q , $|e|$) on individual atom of phenol in gas phase and on the (111) facet of NiMoP catalyst

atom	gas phase	NiMoP
C ₁	+0.39	+0.66
C ₂	+0.06	+0.04
C ₃	- 0.12	- 0.11
C ₄	+0.002	+0.02
C ₅	- 0.09	- 0.12
C ₆	- 0.12	+0.04
O	- 1.16	- 1.14
H	+0.66	+0.64

Table S11: Activation energy barriers (E_A , eV) of main elementary reaction steps involved in DDO reaction mechanism for (112) and (111) facet of NiMoP catalyst by using optB88-vdW functional

reaction step	(112) plane	(111) plane
C-O cleavage	0.8	0.77
ring rotation	0.28	0.28
C-H formation	0.89	0.88

Table S12: Activation energy barriers (E_A , eV) of main elementary reaction steps involved in RH-DO reaction mechanism for phenol (C_6H_5OH) on (112) and (111) facet of NiMoP catalyst by using optB88-vdW functional

reaction step	(112) plane	(111) plane
C ₁ -H formation	0.21	0.17
C ₂ -H formation	0.12	0.09
C ₃ -H formation	0.04	0.05
C ₄ -H formation	0.08	0.05
C ₅ -H formation	0.12	0.1
C ₆ -H formation	0.07	0.05
C ₆ -O cleavage	0.14	0.12